

Temperature-programmed desorption for the characterization of oxide catalysts

R.J. Gorte¹

Department of Chemical Engineering University of Pennsylvania, Philadelphia, PA 19104-6393, USA

Abstract

The application of temperature-programmed desorption (TPD) to the characterization of porous, oxide catalysts is discussed. First, the theory underlying TPD from porous materials is presented briefly and used to demonstrate that adsorption energetics are difficult to measure using TPD. Then, arguments are made that TPD of reactive probe molecules, especially when used in vacuum with controlled exposures, provides much more useful information about the catalyst, including site densities of the active phase of supported oxide catalysts and reaction pathways. Several examples from the literature are used in demonstration of this fact, including the determination of titania surface area in silica-supported titania catalysts, the determination of Brønsted-acid site densities in solid acids, and the elucidation of the reaction intermediates for the reaction of 2-propen-1-ol in an H-ZSM-5 zeolite.

1. Introduction

Temperature-programmed desorption (TPD) is a very powerful technique for characterizing oxide catalysts and determining reaction pathways on oxides. (Note: Depending on the technique used to detect desorption and the particular application, TPD is sometimes called thermal desorption spectroscopy (TDS), TP mass spectroscopy (TPMS), flash desorption, and other names. In this review, the term TPD will be used even when the adsorbate undergoes reaction prior to desorption.) TPD is a relatively inexpensive and simple experiment to set up and run. The sample is placed in either a vacuum chamber or a tube through which an inert

gas can flow. Following exposure to the adsorbate of interest, the temperature of the sample is ramped, usually with a constant heating rate, and the partial pressure of the gas above the sample is measured as a function of temperature.

Compared to many other analytical techniques, TPD provides information which is closely related to the catalytic properties and the reactions in question. With the proper choice of probe molecule, it is frequently possible to relate TPD curves to the catalytic activity and selectivity of a particular catalyst and to determine the probable state of the catalyst under working conditions. Surprisingly, many corporate analytical departments are not equipped to carry out TPD measurements. When the technique is available, it is usually used to measure

¹ 215-898-4439 (phone); 215-573-2093 (Fax).

heats of adsorption, such as for ammonia on acid catalysts, an application for which, in the author's opinion, the technique has questionable value [1,2]. While most investigators tend to think of TPD as a means for measuring adsorption enthalpies and desorption activation energies, these parameters are actually very difficult, and sometimes impossible, to extract from TPD. In cases where the energetics of a particular molecule have been measured on similar samples in different laboratories, such as ammonia from H-ZSM-5, the agreement between laboratories is so poor that the adsorption energetics were uncertain to within a factor of two [3]. The problem results from the fact that a unique, mathematical analysis of the desorption process, along with all of the transport processes and readsorption phenomena that occur simultaneously, becomes impossible. The assumptions typically used to analyze the data are often wrong [4]. However, TPD is well suited for measuring adsorbate coverages and initial reaction products, information which is actually more useful.

A complete review of the literature on the use of TPD in catalysis is not the intent of this article and would, in any case, be almost as broad as the field of catalysis itself. Rather, this paper will describe some of the optimal applications of TPD for oxide catalysts through a few brief examples to demonstrate the power of the technique and the best ways to use it.

2. Background

TPD was first described as a quantitative, analytical tool for surface characterization of low-surface-area samples by Redhead [5]. Using a simple material balance, he showed that the pressure in a vacuum chamber is proportional to the desorption rate for *flat* samples when the pumping speed is high enough, the usual case for ultrahigh vacuum systems. Furthermore, using simple assumptions about the desorption kinetics, he showed that it may be possible to

extract adsorption energetics from desorption curves. The desorption activation energy is approximately equal to the heat of adsorption when the activation energy for adsorption is small, the case for many adsorbates, and can be estimated from the desorption peak temperature. Extracting desorption activation energies, in practice, is more complex than described by Redhead due to the fact that desorption can never be described by simple first- or second-order kinetics. Even simple systems, such as CO desorption from single-crystal metals, exhibit complex desorption kinetics due to molecular interactions [6]. (Note: The common practice of letting the rate constant be coverage dependent implies that the rate is not a simple, n th-order process.) However, there are methods, such as the use of variable sample heating rates [6], which provide unambiguous measurement of activation energies. There are even examples in the literature where heats of adsorption have been determined as a function of coverage for rather complex kinetic rate expressions [7].

The application of TPD to typical, high-surface-area catalysts was first discussed by Cvetanovich and Amenomiya [8]. Usually, but not always, desorption from these types of materials is carried out in a carrier gas, with some kind of detector used to measure the concentration of the gas leaving the sample compartment. Cvetanovich and Amenomiya recognized that the partial pressure is not directly related to the intrinsic desorption rate under these conditions and analyzed the results with several limiting circumstances. Most important for this discussion, they considered the cases where adsorption and desorption are in local equilibrium and where diffusion limits the desorption process. Unfortunately, their mathematical description of diffusion was inadequate for the usual physical situation in which desorption and adsorption are occurring simultaneously with diffusion. As a result, many of their conclusions are incorrect. For example, they stated that increasing the flow rate of the carrier gas could limit the importance of readsorption, and even allow

readsorption to be neglected, a conclusion which can easily be shown to be wrong [4].

A better mathematical description of desorption from porous catalysts was developed by Herz, et al. [9], whose equations considered simultaneous desorption, adsorption, and diffusion from a catalyst pellet, which in turn was inside a CSTR with a carrier gas flushing adsorbate from the cell. Using typical physical parameters, they demonstrated that the peak maximum in the TPD curve could shift by hundreds of degrees due to readsorption, coupled with diffusion, even when the sample was placed in ultrahigh vacuum. Proof that their calculations were valid came from their experimental observations for CO from supported Pt catalysts. The equations developed by Herz, et al. were later nondimensionalized and the effect of various experimental parameters analyzed, first by Gorte [4] and then by Demmin and Gorte [10]. This analysis, which further extended the desorption model to consider the catalyst as making up a packed bed through which the carrier gas passes, resulted in six dimensionless groups of measurable experimental variables. The dimensionless groups, which can be thought of as ratios of characteristic rates in the system, are listed in Table 1. A complete discussion of the implications of each parameter and what the partial pressures above the sample actually measure has been given [10]. The number of rate processes which influence desorption for a porous catalyst demonstrate why the pressure above the sample is usually not proportional to the true, intrinsic desorption kinetics. For typical experimental conditions, adsorption and desorption rates are fast compared to diffusion, so that extraction of intrinsic adsorption and desorption rates is impossible. Under vacuum conditions, which are advantageous for many applications as will be discussed later, desorption is, by definition, in the diffusion-limited regime.

To demonstrate how important transport limitations coupled with readsorption can be, consider the hypothetical TPD curve shown in Fig. 1. For this example, the surface is assumed to

Table 1
Important parameters for characterizing TPD in porous materials

Parameter	Ratio
1	$\frac{\varepsilon_B V \beta}{Q}$ Residence time in sample cell Characteristic "time" for heating
2	$\frac{\varepsilon_p R^2 \beta}{D_p}$ Characteristic diffusion time Characteristic "time" for heating
3	$\frac{QR}{\left(\frac{3W}{\rho R}\right) D_p}$ Rate of moles removed by carrier gas Characteristic rate of diffusion
4	$\frac{\alpha \rho k_{ad} R^2}{\pi D_p}$ Characteristic adsorption rate Characteristic rate of diffusion
5	$\frac{\alpha \rho k_{ad} (1 - \varepsilon_B)}{Q/V}$ Characteristic adsorption rate Rate of moles removed by carrier gas
6	$\frac{QL^2}{VD_B}$ Rate of moles removed by carrier gas Rate of mixing in packed bed

These parameters were derived from the equations describing desorption from a packed bed of catalyst particles. The variables making up the parameters are as follows:

ε_B \equiv porosity of the catalyst bed (cm^3/cm^3).

ε_p \equiv porosity of each particle (cm^3/cm^3).

V \equiv Volume of the bed (cm^3).

β \equiv heating rate (K/sec).

Q \equiv carrier-gas flow rate (cm^3/sec).

R \equiv radius of catalyst particles (cm).

D_p \equiv diffusivity in catalyst particle (cm^2/sec).

D_B \equiv dispersion along the catalyst bed (cm^2/sec).

ρ \equiv density of catalyst (g/cm^3).

α \equiv specific surface area (m^2/g).

k_{ad} \equiv adsorption rate constant, $s(RT/2\pi(MW))^{1/2}$ (cm/sec).

W \equiv mass of catalyst bed (g).

L \equiv length of catalyst bed (cm).

consist of identical sites with the desorption rate described by a simple, first-order process, a reasonable preexponential ($10^{12}/\text{s}$), and a constant desorption activation energy (25 kcal/mol). The diffusion coefficient is assumed to be typical of that for Knudsen flow in mesopores and micropores, $0.01 \text{ cm}^2/\text{s}$, and is much larger than that found in catalysts where one expects diffusion to be limiting, such as in molecular sieves. Desorption is pictured as occurring into a vacuum chamber with a pumping speed of 15 liter/s, using a relatively slow heating rate of 6 K/s. The only pathological aspect of the hypothetical system is that half of the sample weight is assumed to consist of

particles which are 100 μm in diameter and half which are 10 μm in diameter.

The TPD curve shows two peaks, separated by almost 100 K, with the peak at higher temperatures resulting from the larger particles and the one at lower temperatures from the smaller particles. While it is true that the conditions used in the calculation of Fig. 1 were chosen to ensure that two peaks would be observed from a simple desorption process, the parameters used in the calculation are physically realistic and demonstrate that even a simple desorption process can result in a complex TPD curve. Since nature almost never obliges by making the surface homogeneous or the desorption process simple, by providing uniform pores throughout the material so that diffusion can be treated with a single constant, or by providing a uniform particle size throughout the sample, calculating the surface energetics from data is clearly risky and usually model dependent. Even qualitative observations about the desorption process on

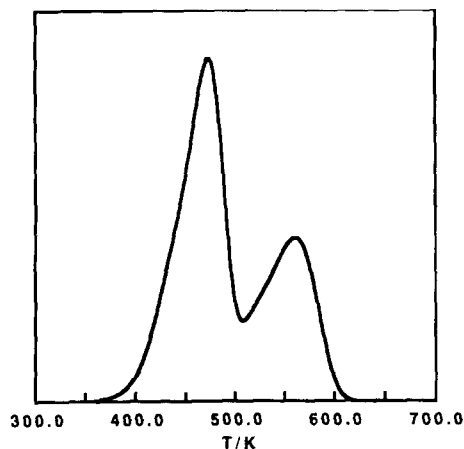


Fig. 1. Calculated TPD curve for desorption from a bed of catalyst, using equations from Ref. [10]. Desorption is assumed to be first order, with a desorption rate constant of $10^{12} \times \exp\{-(25 \text{ kcal/mol})/RT\} \text{ s}^{-1}$. The sample is assumed to be made up of spherical particles, with half the sample mass consisting of particles with a diameter of 100 μm and half with a diameter of 10 μm . Other parameters used in the calculation are as follows: sticking coefficient = 0.1; active surface area = 30 m^2/g ; catalyst density = 1 g/cm^3 ; diffusivity = 0.01 cm^2/sec ; total sample mass = 20 mg; pumping speed = 15 l/sec; heating rate = 6 K/min.

porous materials must be interpreted cautiously (e.g. the two peaks in the TPD curve of Fig. 1 do not imply two types of sites).

Admittedly, it is possible to measure adsorption energetics using TPD under some circumstances, at least if all the sites in the sample are energetically equivalent. Dumesic and co-workers obtained the heat of adsorption for ammonia in a zeolite H-ZSM-5, in good agreement with calorimetric measurements, by measuring TPD curves using different flow rates for the carrier gas [11]. By carefully choosing conditions in which diffusion was not limiting (Parameter 3) in Table 1 is small.), they achieved conditions in which the gas above the sample was in equilibrium with the adsorption sites. By varying the carrier-gas flow rate (within a limited range set by parameter 3) in Table 1.), the equilibrium pressure could be obtained for a given coverage at different temperatures. Finally, the heat of adsorption was calculated from the 'isotherms' and the Clausius–Clapeyron equation. However, this same paper demonstrated that diffusion limitations for pyridine desorption from the zeolite were essentially unavoidable with their experimental setup. Finally, the approach used by these investigators would be difficult to apply in more complex materials in which the heat of adsorption varies with coverage. Given the many other studies of NH_3 desorption in H-ZSM-5 in which dramatically different heats were reported [3], it is not clear that measurement of adsorption energetics is the best application of TPD.

Before describing specific examples of catalytic problems where TPD has been found to provide useful and unambiguous information, two additional points should be made. First, there are significant advantages to using probe molecules which, when adsorbed at catalytic sites, react prior to desorption. This prevents noncatalytic sites from being counted. For example, ammonia is frequently used to titrate acid sites in solid acids; however, ammonia adsorbs strongly on many oxides, including CaO, which are not normally thought to be

acidic. [2] Furthermore, as we have just shown, desorption temperatures, and even the presence of multiple peaks, are determined as much by transport properties as by desorption properties.

Second, for reactive molecules, desorption from small samples in a vacuum is advantageous for minimizing secondary chemistry and migration from noncatalytic sites to catalytic sites. Due to the fact that pore dimensions in typical catalysts are much smaller than the mean-free path of the molecule in the gas phase at pressures near atmospheric, convection (i.e. The ‘forcing’ of molecules out of the sample by means of a carrier gas.) is *always* much slower than removal of desorbing species by evacuation. Even in vacuum, there are no guarantees that readsorption will not complicate the interpretation, as shown in the example in Fig. 1. For purposes of calculating the amounts which desorb from the sample by means of a mass balance on the system, the carrier-gas flow rate is equivalent to the pumping speed of the vacuum system [4,9,10]; and coverages can be determined by integrating the features in the TPD curves, so long as parameter 1) in Table 1 is small [10]. Since typical pumping speeds in vacuum are of order 10 liter/s or higher, compared to 1 ml/s for carrier-gas flow rates, the effect of evacuation on peak temperatures and minimizing secondary reactions, due to the decreased partial pressure of adsorbate above the sample, can be dramatic. For unreactive molecules like NH_3 in H-ZSM-5, a recent example showed that the use of vacuum rather than a carrier gas can shift desorption by more than 150 K [1]. For reactive molecules, a comparison of TPD curves for methanol and acetone from H-ZSM-5 in high vacuum [12,13] and in a carrier gas [14,15] shows that both molecules desorb largely intact in vacuum, but react to a wide range of hydrocarbon products when desorption is carried out using a carrier gas.

In the next sections, several examples will be provided which demonstrate the types of information which can be obtained using TPD on oxides.

3. Optimal uses of TPD: A few examples

3.1. Surface area of catalytic oxides

Selective adsorption is widely used for measuring active surface areas with supported-metal catalysts. For example, with oxide-supported metals like Pt, Rh, or Ni, CO or H_2 adsorbs selectively on the metals and not on the support [16]. Reaction rates are often reported in terms of the metal surface area, or number of sites, since these specific rates are often constant for a given set of reaction conditions.

This is not usually done for oxides, even though many catalytic oxides are supported on a second, inert oxide. Even for acid catalysts, where discrete sites are likely, rates are usually reported in terms of catalyst mass or total, BET surface areas. The primary reason for not reporting rates in terms of active surface areas, or sites, is that determination of these quantities is difficult and frequently ambiguous. TPD appears to provide an excellent method for determining the active surface area. One case where TPD has been successfully applied to measuring specific surface areas is that of titania on silica supports [17,18]. Among other applications, titania silicates can be used as a support for vanadia in selective catalytic reduction of NO_x , in which application it is vital to maximize the surface area of the titania [17]. The methodology used in these studies is also of interest, since the approach can probably be applied to other catalysts as well, if one can find an appropriate probe molecule.

The particular property which allows the surface of titania to be distinguished from that of silica is that titania is a stronger Lewis acid. For adsorption of 2-propanol, this acidity leads to dehydration in TPD at considerably lower temperatures on titania, as demonstrated in Fig. 2 which shows the TPD curves, monitoring only the $m/e = 41$ peak, for pure titania (prepared by precipitation of titanyl sulfate) and pure silica. For this particular titania, dehydration occurs at 200°C, while the peak dehydration tem-

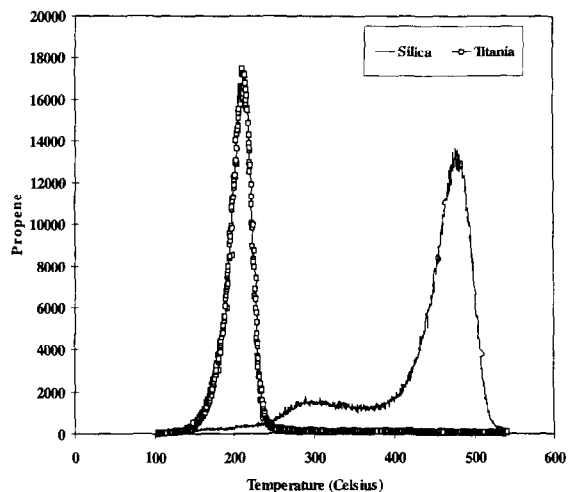


Fig. 2. TPD curves for 2-propanol from titania and silica; only the peak intensity for $m/e = 41$ is shown in arbitrary units. The dramatic difference in the ability of these two oxides to dehydrate 2-propanol can be used to discriminate how much of the surface is covered by titania. (The figure is taken from Ref. [17].)

perature for silica was above 450°C [17]. Swain, et al. examined a whole series of mechanically blended and chemically dispersed, titania silicates in which the chemically dispersed materials were prepared by precipitation of titanyl sulfate in the presence of silica. In each case, the TPD curves were found to show desorption features in the same temperature ranges, with the relative amounts reacting at the lower temperatures corresponding the fraction of the sample that was titania. Based on several other techniques, including measurement of the catalyst activity for NO_x reduction after incorporation of vanadia, the authors of this study concluded that the propene formed at lower temperatures in TPD was an effective measure of the titania surface area. From data reported in their paper, the specific coverage of 2-propanol on titania is approximately 1.8×10^{18} molecules/m².

In the study of Swain et al., the structure of the titania in the mixed oxides was likely to be very similar to pure titania because of the way in which the samples were made. Obviously, other methods of preparation could lead to materials with different reactivities and specific

coverages for the alcohol [19]. While these complications must be recognized, the general approach still appears to work, even for monolayer forms of titania on silica [18]. In conclusion, TPD measurements with 2-propanol on titania silicates appear to be a very useful method for determining the surface areas of the titania component. The amount of 2-propanol which reacts at lower temperatures in TPD is proportional to the surface area of the titania, while 2-propanol interacts much more weakly on the silica.

3.2. Determination of Brønsted-acid sites

The most useful probe molecules for measuring Brønsted-acid, site concentrations are simple alkyl amines, other than methylamine. These molecules are protonated to form ammonium ions by the acid sites and decompose, via a reaction similar to the Hoffman elimination, to olefin and ammonia products [2,13]. (Methylamine is not a good probe molecule because it cannot decompose to an olefin product without at first going through a bimolecular reaction [20].) The strength of the acid site does not influence the temperature at which decomposition of the amine takes place, which implies that the reactivity of the alkylammonium ion is not strongly influenced by the solid anion but is simply a function of the alkylammonium ion itself. Because the reaction temperature is relatively high, above 575 K for isopropylamine, 'physisorbed' species and molecules adsorbed at Lewis sites have left the sample prior to the decomposition event, preventing the overcounting of sites by readsorption of amines from noncatalytic sites to the Brønsted sites.

Typical results for a TPD-TGA measurement of isopropylamine in an H-ZSM-5 zeolite are shown in Fig. 3. H-ZSM-5 is an ideal sample for demonstrating the technique because it contains one Brønsted-acid site for each framework Al. In Fig. 3, this 1:1 adsorption complex is clearly visible as the desorption of propene and ammonia between 575 and 650 K.

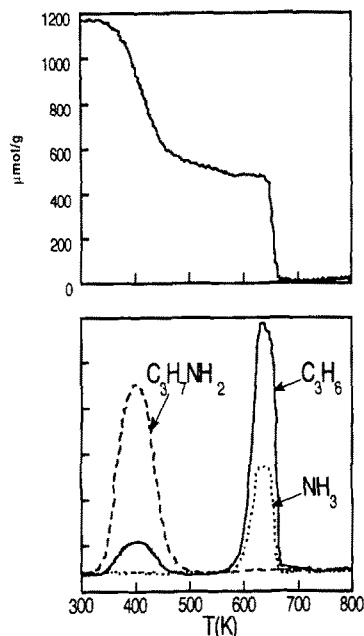


Fig. 3. TPD–TGA curves for isopropylamine from an H-ZSM-5 catalyst containing approximately 500 $\mu\text{mol/g}$ of Brønsted-acid sites. A mass spectrometer was used to determine the products, with signals for isopropylamine ($m/e = 30$ and 41), propene ($m/e = 41$), and ammonia ($m/e = 17$).

TGA indicates that the amount desorbing from this region is close to the Al content of the sample. The amount of unreacted amine desorbing at lower temperatures, below 500 K in Fig. 3, depends on the evacuation time, the pumping speed, and the particular sample; however, the 1:1 adsorption complex is relatively unaffected by the experimental parameters used in the study. The technique works equally well for amorphous silica–aluminas [21], fluid-catalytic cracking catalysts [22], and sulfonated zirconias [23]. It is insensitive to Lewis-acid sites [2,21,24]. Furthermore, the concentrations one obtains for a given material are insensitive to the particular amine which is chosen to probe the sites, so long as the sites are physically accessible to the amine [25].

Finally, it should be noted that the amine desorption technique is extremely sensitive to very small Brønsted-site concentrations, having been used to quantify site densities down to 2 $\mu\text{mol/g}$ [26], a site density equivalent to an

H-ZSM-5 catalyst with a Si/Al₂ ratio of $\sim 16,000$. Given the high sensitivity of this technique, and its ability to discriminate between Brønsted- and Lewis-acid sites, it would appear that TPD of amines should find wide application to the characterization of solid acids. [2]

3.3. Cu exchange in ZSM-5

In the case of Cu exchange in high-silica zeolites, one again forms discrete sites with unique catalytic properties [27]. Quantification of these sites can again be determined by TPD measurements of amines [28,29]. The chemistry in this case is quite different from the Hoffman elimination found with acidic materials, but well-defined, stoichiometric adsorption complexes are again distinguishable by the unique chemistry observed at these sites. Due to similarities in the approach to that used for determining Brønsted-acid sites, the details will not be discussed here. However, the fact that one can identify different types of sites with TPD, from Cu-exchanged sites to Brønsted-acid sites to titania sites, does suggest that the approach is quite general and can probably be applied to a range of catalytic materials, including oxidation catalysts [26].

3.4. 2-Propen-1-ol in H-ZSM-5

TPD is also useful for gaining information about reaction mechanisms, and an interesting example for demonstrating this is that of 2-propen-1-ol (allyl alcohol) in H-ZSM-5 [30]. In addition to showing the type of information that can be gained, this example demonstrates some of the difficulties that one can encounter in the study of the adsorption of reactive molecules and the utility of combining TGA with mass spectral analysis of the gas-phase species. The example also demonstrates that great care must be used during adsorption of reactive molecules in order to avoid missing the important chemistry during the initial exposure of the catalyst. The steady-state reaction of allyl alcohol in

H-ZSM-5 is quite complex. A wide variety of products can be formed, from aldehydes to aromatics, depending on the reaction conditions which include the catalyst time on stream [31]. Ascertaining the reaction mechanisms from the reaction products is therefore very difficult.

TPD–TGA curves for 2-propen-1-ol on H-ZSM-5 following high and low initial exposures are shown in Fig. 4 and Fig. 5. In Fig. 4, the zeolite was saturated briefly with 2-propen-1-ol using 10 torr of vapor and then evacuated for two hours [30]. The coverage after evacuation was still two molecules/site. (While determination of all products formed in TPD is nontrivial from the mass spectral data due to the complex fragmentation patterns of most hydrocarbons, a

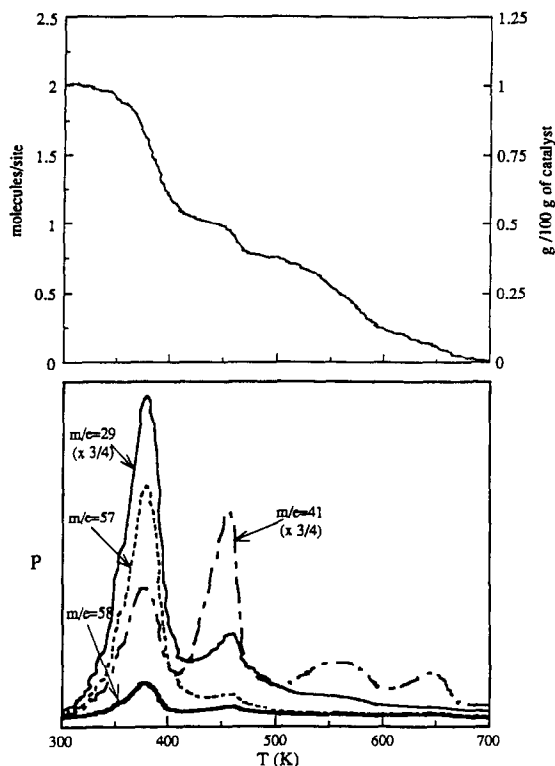


Fig. 4. TPD–TGA curves for 2-propen-1-ol in H-ZSM-5 following a saturation exposure. The peaks in the mass spectrum correspond to 2-propen-1-ol ($m/e = 29, 57, 41,$ and 58) and olefins ($m/e = 41$). Only those molecules in excess of one per site desorb unreacted, with significant condensation reactions occurring for the molecules at the acid sites. (Figure taken from Ref. [30].)

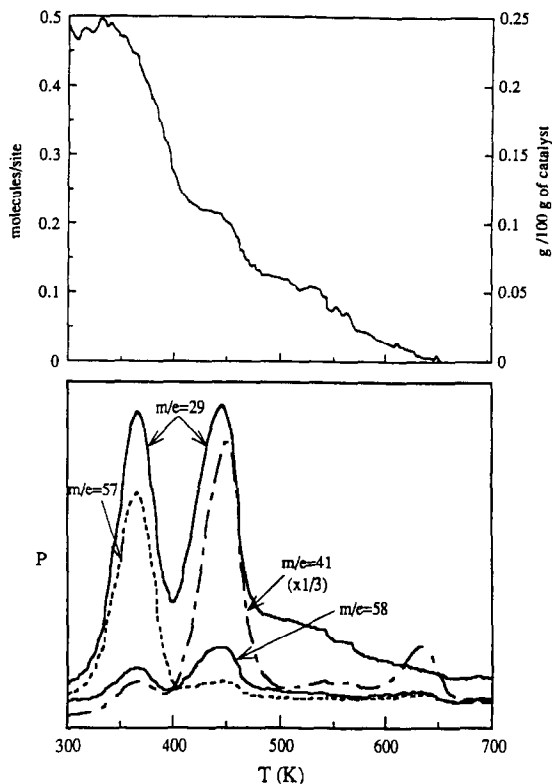


Fig. 5. TPD–TGA curves for 2-propen-1-ol in H-ZSM-5, following a low (< 1 molecule/site) initial exposure. The peaks in the mass spectrum correspond to 2-propen-1-ol ($m/e = 29, 57, 41,$ and 58), propanal ($m/e = 29, 58,$ and 57) and olefins ($m/e = 41$). Differences between these results and those shown in Fig. 4 demonstrate how important are the conditions at which the catalyst is exposed to the adsorbate. (Figure taken from Ref. [30].)

preliminary scan of the entire mass spectrum at regular temperature intervals allowed most of the initial products to be identified. More definitive identification required the products to be collected in a trap for analysis by chromatography [32].) Some of the 2-propen-1-ol ($m/e = 29, 57, 41,$ and 58) above a coverage of one molecule/Brønsted site desorbs from the sample below 400 K; however, essentially all of the molecules at the acid sites react. Beginning at ~ 425 K, a number of hydrocarbon products are observed, all exhibiting a peak at $m/e = 41$ in their mass spectrum. Analysis by gas chromatography showed that the products include a range of olefins and aromatics [32] as complex as that observed in the steady-state reaction.

The importance of carrying out the measurement in a microbalance is demonstrated by the fact that the sample weight did not return to its initial value, even after heating to 750 K, indicating that some coke is formed in the sample.

The results for a low exposure are quite different. For the TPD–TGA curves shown in Fig. 5, 2-propen-1-ol was slowly dosed onto the sample while monitoring the sample weight. Dosing was stopped before reaching a coverage of one/site. While about half of the 2-propen-1-ol leaves the sample below 400 K, as shown by the fragmentation pattern in the mass spectrum, the first product formed in the reaction, between 400 and 475 K, is propanal. (The relative intensities of the $m/e = 57$ and 58 peaks are reversed for 2-propen-1-ol and propanal, even though they have identical molecular weights.) At higher temperatures, one starts to observe other hydrocarbon products, including aromatics and other olefins.

The observation that propanal is the first product formed by the unimolecular reaction of 2-propen-1-ol at the acid sites of H-ZSM-5 lead to a further study of adsorption of propanal [30]. Not surprisingly, saturation of the zeolite with propanal gave very similar products to that observed for 2-propen-1-ol in TPD. Furthermore, ^{13}C NMR showed that similar surface species were formed following the adsorption of propanal and 2-propen-1-ol. Therefore, reactions of 2-propen-1-ol in the zeolite appear to proceed through the aldehyde, and aldol-condensation reactions are largely responsible for the products which are formed.

Clearly, the observation of propanal in the TPD measurements was instrumental in identifying this reaction pathway. Unfortunately, it was necessary to control the exposure of 2-propen-1-ol in order to see this initial product; and additional reactions of the propanal tended to mask the observation of the initial product. It is for these reasons that working in vacuum, rather than a packed tube through which a carrier gas is passed, is so important. Even in vacuum, bimolecular reactions are difficult to avoid.

3.5. Alcohols, thiols, and olefins in H-ZSM-5

While the example of 2-propen-1-ol is good for showing the utility of TPD because the reaction is relatively complex and a number of reaction pathways are feasible, there are other examples which show how much information on reactions can be obtained from TPD. Information on the dehydration of alcohols [12], on hydrodesulfurization of thiols [33], and on the oligomerization of ethene and propene [34] has also been obtained using TPD. TPD was particularly useful for explaining the nature of olefin oligomerization in zeolites and the difficulty of obtaining simple products in this reaction. However, it is not the purpose of this paper to review all applications where TPD has been instrumental in understanding a particular reaction, but rather to demonstrate the types of information that can be obtained. The reader should realize that TPD can and has been used in a wide variety of other reactions. Hopefully, even more laboratories will take advantage of TPD for understanding surface-catalyzed reactions.

4. Summary

TPD is a powerful technique, with widely ranging applications for determining site densities and elucidating reaction pathways on typical oxide catalysts. However, while TPD is often applied to measuring adsorption energetics, the complexity of desorption from porous catalysts suggests that TPD is not well suited for this. The best ways of using TPD are still being developed; and, given the relative simplicity and low cost of the technique, TPD will almost certainly continue to find more applications in the future.

Acknowledgements

Most of the work described in this paper was supported by the NSF, Grant CTS94-03909.

The help of Mr. Chi Lee and Mr. Harry Cordatos in preparing the manuscript is gratefully acknowledged.

References

- [1] See Fig. 2 in W.E. Fameth and R.J. Gorte, *Chem. Rev.*, 95 (1995) 615.
- [2] M.V. Juskelis, J.R. Slanga, T.G. Robed and A.W. Peters, *J. Catal.* 138 (1992) 391.
- [3] E.H. Teunissen, R.A. van Santen, A.P.J. Jansen and F.B. van Duijneveldt, *J. Phys. Chem.*, 97 (1993) 203.
- [4] R.J. Gorte, *J. Catal.*, 75 (1982) 164.
- [5] P.A. Redhead, *Vacuum*, 12 (1962) 203.
- [6] J.L. Falconer and R.J. Madix, *Surf. Sci.*, 48 (1975) 93.
- [7] H. Pfnür, R. Feulner, H.A. Engelhardt and D. Menzel, *Chem. Phys. Lett.*, 59 (1978) 481.
- [8] R.J. Cvetanovic and Y. Amenomiya, *Advan. Catal.*, 17 (1967) 103.
- [9] R.K. Herz, J.B. Kiela, S.P. Marin, *J. Catal.*, 73 (1982) 66.
- [10] R.A. Demmin, R.J. Gorte, *J. Catal.*, 90 (1984) 32.
- [11] S.B. Sharma, B.L. Meyers, D.T. Chen, J. Miller and J.A. Dumesic, *Appl. Catal. A*, 102 (1993) 253.
- [12] M.T. Aronson, R.J. Gorte and W.E. Fameth, *J. Catal.*, 98 (1986) 434.
- [13] T.J.G. Kofke, R.J. Gorte and W.E. Fameth, *J. Catal.*, 114 (1988) 34.
- [14] J. Novakova, L. Kubelkova and Z. Dolejsek, *J. Catal.*, 108 (1987) 208.
- [15] J. Novakova, V. Bosacek, Z. Dolejsek and L. Kubelkova, *J. Mol. Catal.*, 78 (1993) 43.
- [16] L. Spenadel and M. Boudart, *J. Phys. Chem.*, 64 (1960) 204.
- [17] J.E. Swain, M.V. Juskelis, J.R. Slanga, J.G. Miller and M. Uberoi, *Appl. Catal. A*, 109 (1996) 175.
- [18] A.I. Biaglow, R.J. Gorte, S. Srinivasan and A.K. Datye, *Catal. Lett.*, 13 (1992) 313.
- [19] Z.F. Liu and R.J. Davis, *J. Phys. Chem.*, 98 (1994) 1253.
- [20] D.J. Parrillo, A.T. Adamo, G.T. Kokotailo and R.J. Gorte, *Appl. Catal.*, 67 (1990) 107.
- [21] J. Tittensor, R.J. Gorte and D. Chapman, *J. Catal.*, 138 (1992) 714.
- [22] A.I. Biaglow, C. Gittleman, R.J. Gorte and R.J. Madon, *J. Catal.*, 129 (1991) 88.
- [23] K.T. Wan, C.B. Khouw and M.E. Davis, *J. Catal.*, 158 (1996) 311.
- [24] A.I. Biaglow, D.J. Parrillo, G.T. Kokotailo and R.J. Gorte, *J. Catal.*, 148 (1994) 213.
- [25] C. Pereira and R.J. Gorte, *Appl. Catal.*, 90 (1992) 1.
- [26] V. Kurshev, L. Kevan, C. Perelm, D.J. Parrillo, G.T. Kokotailo and R.J. Gorte, *J. Phys. Chem.*, 98 (1994) 10160.
- [27] V. Kanazirev, G.L. Price and K.M. Dooley, *Catal. Lett.*, 24 (1994) 227.
- [28] D.J. Parrillo, D. Dolenc, R.J. Gorte and R.W. McCabe, *J. Catal.*, 142 (1993) 708.
- [29] D.J. Parrillo, J.R. Fortney and R.J. Gorte, *J. Catal.*, 153 (1995) 190.
- [30] A.I. Biaglow, J. Sepa, R.J. Gorte and D. White, *J. Catal.*, 154 (1995) 208.
- [31] G.I. Hutchings, D.F. Lee and C.D. Williams, *J. Chem. Soc. Chem. Comm.*, 1475 (1990).
- [32] C. Pereira, G.T. Kokotailo, R.J. Gorte and W.E. Fameth, *J. Phys. Chem.*, 94 (1990) 2063.
- [33] C. Pereira and R.J. Gorte, in R. von Ballmoos, J.B. Higgins, M.M.J. Treacy, Editors, *Proc. 9th Intern. Zeol. Conf.*, Vol. 2, Butterworths, 1993 p. 243.
- [34] T.J.G. Kofke and R.J. Gorte, *J. Catal.*, 115 (1989) 233.